Physica B: Condensed Matter 555 (2019) 69–73

Contents lists available at ScienceDirect

Physica B: Condensed Matter

journal homepage: www.elsevier.com/locate/physb

Modulation of electronic properties and Schottky barrier in the graphene/GaS heterostructure by electric gating

Khang D. Pham[a,b], Hieu Vu-Quang[c], Chuong V. Nguyen[d,*]

[a] Laboratory of Applied Physics, Advanced Institute of Materials Science, Ton Duc Thang University, Ho Chi Minh City, Viet Nam
[b] Faculty of Applied Sciences, Ton Duc Thang University, Ho Chi Minh City, Viet Nam
[c] NTT Hi-Tech Institute, Nguyen Tat Thanh University, Ho Chi Minh City, Viet Nam
[d] Department of Materials Science and Engineering, Le Quy Don Technical University, Ha Noi, Viet Nam

ARTICLE INFO

Keywords:
Graphene
Gallium sulfide
Electric gating
Schottky barrier

ABSTRACT

In this work, the structure, electronic properties, and the Schottky barrier of the van der Waals heterostructure (vdWH) based on graphene and gallium sulfide (GaS) have been theoretically considered using density functional theory. We found that the graphene/GaS vdWH keeps the extraordinary intrinsic properties of both the graphene and GaS monolayer. Moreover, an *n*-type Schottky contact with a small Schottky barrier of 0.51 eV was formed in the ground state of the heterostructure. Especially, our results demonstrated that applying an electric gating can tune effectively the Schottky barrier and contact types. The transformations from the *n*-type Schottky contact to the *p*-type one and from the Schottky to the Ohmic contacts were observed in the vdWH under electric gating. These results propose a great potential for the van der Waals heterostructure in future nanoelectronic and optoelectronic devices.

1. Introduction

Recently, graphene-like two-dimensional (2D) materials are being intensively considered because of their extraordinary electronic, optical and transport properties, which are suitable for designing high-performance devices in nanoelectronics and optoelectronics [1–3]. Graphene is well-known as a 2D sp^2–hybridized carbon material. It has been widely focused due to its remarkable properties and fascinating potential applications [4,5]. However, graphene has a zero band gap, which has restricted its wide application, for instance in high-speed electronic devices [6]. To date, many potential 2D materials such as transition metal dichalcogenides [7–10], phosphorene [11–14], layered group–III monochalcogenides [15–17] have been investigated widely because of their remarkable physical properties and promising applications for nano- and optoelectronic devices. Among these, monolayer GaS, a stable class of 2D metal dichalcogenides, has recently been synthesized experimentally by the vapor–solid method [18], opening its fascinating applications. Soon after, theoretical investigation from first-principles calculations have shown that monolayer GaS is a semiconductor with an indirect band gap of 2.48 eV/3.19 eV, given from PBE/HSE06 calculations [19]. These investigations make monolayer GaS promising candidate in future electronic devices such as field-effect transistors (FETs) [20].

More recently, van der Waals heterostructures (vdWHs) based on graphene and other 2D materials layer by layer are being considered widely. Especially, many graphene–vdWHs such as graphene/MoS_2 [21,22], graphene/GaSe [23,24] and so on, have been realized experimentally. For instance, Roy et al. [21] demonstrated photodetectors based on the graphene/MoS_2 heterostructure with a high responsivity of 5×10^8 AW^{-1} at room temperature. Lu et al. [25] demonstrated that high gain and fast photoresponse can be achieved simultaneously in the graphene/GaSe heterostructure, making it suitable for designing graphene-based phototransistors. These findings demonstrated that the graphene-based vdWHs can be used for designing next-generation nanodevices. At the same time, the physical properties of different graphene-based vdWHs, such as graphene/MoS_2 [26], graphene/phosphorene [27,28], graphene/GaSe [29,30] and so on, have been already investigated theoretically. One can observe that in these graphene-based vdWHs, the graphene layer is bonded to 2D materials by the weak vdW interactions and without any dangling bonds. Thus, their intrinsic electronic properties are preserved in the vdWHs. Moreover, it can be seen that these graphene-based vdWHs show many more new interesting properties, which are ideal properties to be applied in nanoelectronics and optoelectronics.

To date, the combination of the graphene and other layered group–III monochalcogenides such as graphene/InSe [31–33],

* Corresponding author.
E-mail addresses: phamdinhkhang@tdtu.edu.vn (K.D. Pham), chuong.vnguyen@lqdtu.edu.vn (C.V. Nguyen).

https://doi.org/10.1016/j.physb.2018.11.049
Received 21 August 2018; Received in revised form 18 November 2018; Accepted 22 November 2018
Available online 23 November 2018

graphene/GaSe [25,29,30] has received considerable interest in both theoretical and experimental studies. All these findings suggest that stacking the graphene layer on top of another layered group–III monochalcogenides into vdWHs provides an effective way to design novel compounds with promising properties. This motivates us to consider the combinations between graphene and layered group-III monochalcogenide GaS monolayer, and also to check whether they can form a stable graphene/GaS vdWH and what interesting electronic properties it can provide as well as the effect of an electric gating. Therefore, in this work, we have a bold idea to construct an ultra-thin graphene/GaS vdWH by means of density functional theory (DFT). We then investigate the electronic properties and Schottky contact of the graphene/GaS vdWH without and with applied electric gating.

2. Computational model and methods

In the present study, first-principles calculations based on DFT method, which is implemented in Quantum Espresso package [34], are used to perform the geometric optimization and electronic properties calculations. The projected augmented wave (PAW) method [35], Perdew, Burke, and Ernzerhof (PBE) [36] parametric of the generalized gradient approximation (GGA) were used to describe the exchange-correction functional. For the long vdW bonding in the vdWH, we opt for Grimme's DFT-D2 method, which has been applied to describe the long-range weak vdW interaction [37]. The energy cut-off was set to 500 eV, and $10 \times 10 \times 1$ k-point grid is selected in the Brillouin zone (BZ) integration. Each geometric optimization was performed when the total energy and the forces are converged to be 10^{6} eV and 10^{-3} eV/Å, respectively. In addition, we used a large vacuum layer thickness of 20 Å along the z direction to break the interactions between adjacent layers.

3. Results and discussion

Before designing the graphene/GaS vdWH, we first check the crystal structure and electronic properties of the individual pristine graphene and monolayer GaS. In Fig. 1, we display the atomic structures and band structures of pristine graphene and GaS monolayer at the ground state. It indicates that the lattice constant of the graphene and GaS monolayer, respectively, is 2.461 Å and 3.585 Å, which are in good agreement with previous calculations [17,38]. In addition, it is shown that graphene has a zero band gap in its pristine form, revealing its metallic character, as illustrated in Fig. 1(b). Unlike graphene, the GaS monolayer is a semiconductor with an indirect band gap of 2.56 eV. This band gap of the GaS monolayer shown in Fig. 1(d) is formed by the conduction band minimum (CBM) at the Γ point and the valence band maximum (VBM) at the Γ–M path.

We now design an ultra-thin G/GaS vdWH by stacking the G layer on top of the monolayer GaS layer-by-layer, as shown in Fig. 2(a and b). To design this vdWH, we use a (2×2) supercell of monolayer GaS, containing 8 gallium atoms and 8 sulfide atoms, and a (3×3) supercell of the G, containing 18 carbon atoms. In addition, we also considered the G/GaS vdWH with a 30° twist angle by rotating the upper G layer 30° about the z direction with the under layer GaS fixed, but the calculated binding energy is much larger than that of without rotation. It is well known that the lower value of the binding energy, the more stable structure of the heterostructure. Hence, in this work, we only choose the most stable structure as an object of the concrete research. In such G/GaS vdWH, one carbon atom is located directly above the gallium atom, and another one is located above the sulfide atom. After geometric optimization, we can obtain the interlayer spacing between the G layer and the GaS layer, that is 3.356 Å. Interestingly, this value of the interlayer spacing is similar to that of other graphene-based vdWHs, such as graphene/GaSe [24,30,39], graphene/SnS_2 [40], graphene/GaN [28,41], which are the typical representatives of the graphene-based vdWHs. So, it indicates that the weak vdW interactions are

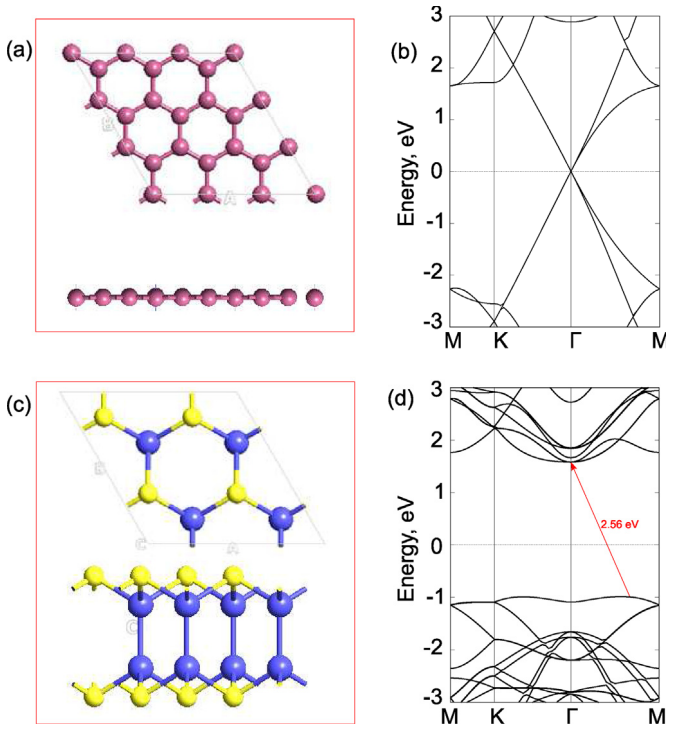

Fig. 1. Top and side views (a) and band structure (b) of the freestanding graphene. Top and side views (c) and band structure (d) of the isolated GaS monolayer. The Fermi level is set to be zero. The pink, dark-blue, and yellow colors stand for carbon, gallium, and sulfide, respectively. (For interpretation of the references to color in this figure legend, the reader is referred to the Web version of this article.)

dominated between the G layer and GaS monolayer in the heterostructure.

In order to verify the structural stability, the binding energy per carbon atom (BE/C) in the graphene/GaS vdWH as a function of the interlayer spacings is also calculated as follows: $E_b = (E_H - E_G - E_{GaS})/N$, where E_H, E_G, and E_{GaS} respectively are the total energy of the vdWH, freestanding graphene, and isolated GaS monolayer. $N = 18$ is the number of carbon atoms in the vdWH. At the ground state, the BE/C in the vdWH is calculated to be -2.5 meV, and it increases with increasing the interlayer spacings, as shown in Fig. 2(c). Besides, according to the obtained equilibrium interlayer spacing and the negligible BE/C, it is obvious that the weak vdW interactions are dominated in the G/GaS vdWH, similar to other graphene-based vdWHs [24,28,30,39–41].

Fig. 2(d) shows the vdWH band structure, which seems to be the sum of that of freestanding G and monolayer GaS, as compared with those of the pristine G and monolayer GaS shown in Fig. 1(b) and (d). The linear dispersion at the Dirac point of the graphene is well kept in the graphene/GaS vdWH, whereas, the monolayer GaS keeps an indirect semiconductor with the CBM at the Γ point and the VBM at the Γ–M path. The nature of this behavior is due to the weak vdW interaction, which not strong enough to modify the energy band morphology of graphene. Thus, the linear dispersion at the Dirac point around the Fermi level of graphene is still preserved in the vdWH, and its Fermi level is located exactly at the Dirac point. These results demonstrate the intrinsic extraordinary properties, holding by graphene and GaS monolayer are preserved in the vdWH.

Interestingly, the G/GaS vdWH represents a metal/semiconductor heterostructure. In practice, the Schottky barrier of the metal/semiconductor heterostructure is an important factor in determining the device performance. Thus, in the considered here G/GaS vdWH, it is necessary to establish its Schottky barrier height (SBH), which can be

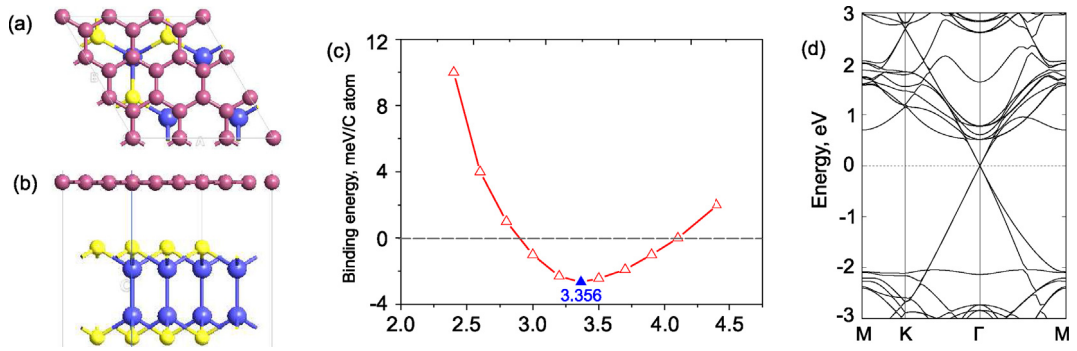

Fig. 2. (a) Top and (b) side views, (c) band structure of the G/GaS vdWH at the equilibrium state. (d) Binding energy per carbon atom of the G/GaS vdWH as a function of the interlayer distance *d*. The pink, dark-blue, and yellow colors stand for carbon, gallium, and yellow, respectively. The Fermi level is set to be zero. (For interpretation of the references to color in this figure legend, the reader is referred to the Web version of this article.)

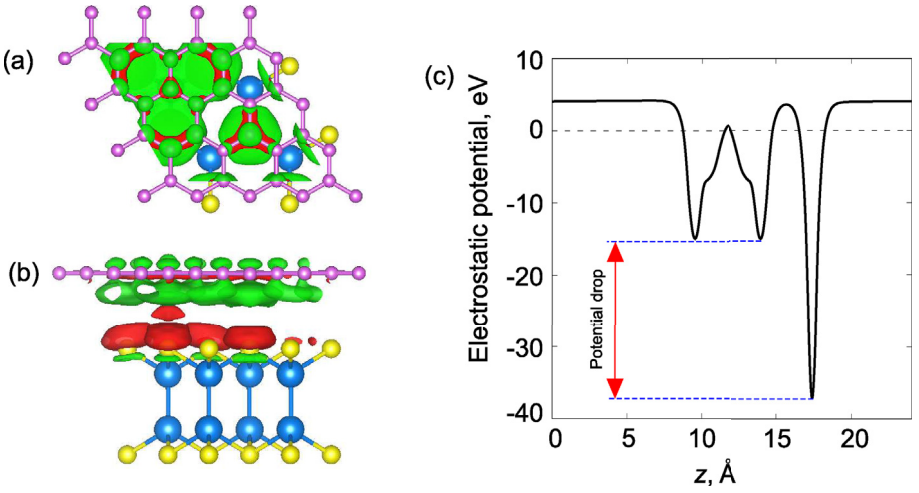

Fig. 3. (a) The charge density difference and (b) the electrostatic potential of the graphene/GaS vdWH at the equilibrium state. The red and green colors correspond to the accumulation and depletion of electron densities. (For interpretation of the references to color in this figure legend, the reader is referred to the Web version of this article.)

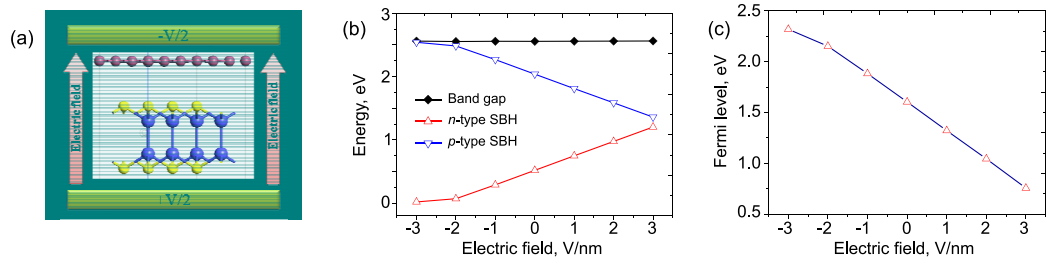

Fig. 4. (a) The schematic diagram of the graphene/GaS heterostructure with the electric field applied perpendicularly to its surface. The variation of (b) the Schottky barrier height and (c) the Fermi energy level of the graphene/GaS vdWH as a function of applied electric field.

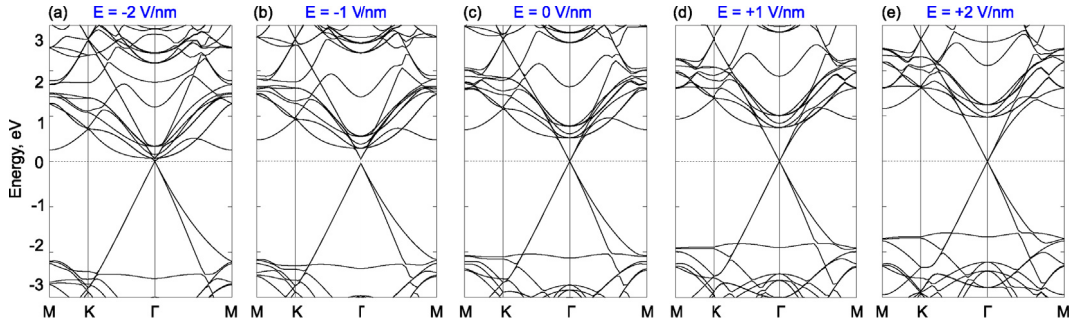

Fig. 5. Band structures of the graphene/GaS vdWH under different strength of applied electric field of (a) −2 V/nm, (b) −1 V/nm, (c) 0 V/nm, (d) +1 V/nm, and (d) +2 V/nm, respectively. The Fermi level is set to be zero.

defined via the Schottky-Mott model [42]. The *n*-type SBH can be described as $\Phi_{Bn} = E_{CBM} - E_F$, where E_F is the Fermi energy level. And, the *p*-type SBH is $\Phi_{Bp} = E_F - E_{V\ BM}$. Our results show that the vdWH forms an *n*-type Schottky contact with the SBH of 0.51 eV.

In Fig. 3(a), we display the visualization of the charge density difference (CDD) to examine the charge transfer in the vdWH. The CDD in the vdWH can be defined as: $\Delta\rho = \rho_H - \rho_G - \rho_{GaS}$, where ρ_H, ρ_G, and ρ_{GaS} respectively are the charge densities of the graphene/GaS vdWH, graphene, and monolayer GaS. The red and green regions represent charge accumulation and depletion in the graphene/GaS vdWH, respectively. We find that the charge accumulates around the topmost sulfide layer of the monolayer GaS, whereas the charge depletion occurs around the graphene layer. This finding also indicates the weak vdW interaction dominated between the graphene layer and monolayer GaS in the vdWH. Fig. 3(b) shows the electrostatic potential in the graphene/GaS vdWH and demonstrates that the GaS monolayer has a higher electrostatic potential than that of the graphene layer, leading to an induced built-in electric field in the vdWH. Moreover, it also suggests that electrons are transferred easily from the monolayer GaS to the graphene layer in the vdWH.

We now consider the effect of electric gating on the electronic properties and the Schottky barrier of the heterostructure. In Fig. 4(a) we show the schematic diagram of the applied electric gating along the *z* direction of the G/GaS vdWH. The positive direction of the electric field is defined to be the direction from the GaS monolayer to the G layer. Fig. 4(b) displays the dependence of the SBH on the strength of the electric gating. We find that both the SBH and contact types in the considered vdWH could be modulated by applying a negative electric gating. First, it is obvious that because of the change in the position of the Fermi energy level under negative electric gating, the SBH of the *n*-type and *p*-type also varies. For instance, the *n*-type SBH decreases linearly with decreasing negative electric gating, while the *p*-type increases. When the negative electric gating is applied, the Fermi level is upshifted from the VBM to the CBM of the GaS part. The *n*-type SBH, in this case, is heightened, while the *p*-type one is reduced. Thus, by applying negative electric gating, the vdWH still keeps an *n*-type Schottky contact. However, when the negative electric field is larger than −3 V/nm, a transition of the contact type from Schottky to Ohmic is observed in such vdWH, i.e its *n*-type SBH is a negative value. In contrary, applying the positive electric gating results in a decrease in the *p*-type SBH and in an increase in the *n*-type SBH, as shown in Fig. 4(b). There appears a transformation from the *n*-type Schottky contact to the *p*-type one when applying electric gating is larger than +3 V/nm. For instance, the *p*-type SBH of the vdWH under electric gating of 3.5 V/nm is 1.36 eV, which is larger than that of the *n*-type one of 1.22 eV. The reason for these changes can be understood by analyzing the position of the Fermi level at the equilibrium state and under the electric gating, as shown in Fig. 4(c). We find that more electrons flow to the G layer from the GaS monolayer, leading to the shift in the position of the Fermi level from the VBM to the CBM.

We further calculate the band structures of the vdWH under the different strength of the electric field, as shown in Fig. 5. As discussed above, by applying a negative electric field, the position of the Fermi level moves from the VBM to the CBM of the GaS monolayer in the heterostructure, resulting in a decrease/increase in the *n*-type/*p*-type SBH. When the applied negative electric field is larger than −3 V/nm, the CBM of the GaS part reduces gradually and crosses the Fermi level. The *n*-type SBH, in this case, becomes a negative value, leading to a transformation in the graphene/GaS vdWH from the Schottky contact to the Ohmic one. By applying a positive electric field, the Fermi level shifts downwards from the CBM to the VBM, resulting in an increase/decrease in the *n*-type/*p*-type SBH. When the strength of the positive electric field is larger than +3 V/nm, the *n*-type SBH becomes larger than that of the *p*-type one, leading to a transformation of the Schottky contact from the *n*-type to the *p*-type. Therefore, these results show that in the graphene/GaS vdWH, both the Schottky barrier (*n*-type and *p*-type) and contact types (Schottky or Ohmic contact) can be controlled efficiently by applying an electric field perpendicularly to the heterostructure surface. The reasons of the transformation of Schottky contact (*n*-type and *p*-type) and contact types (Schottky and Ohmic contacts) in the vdWH under electric field are the interfacial charge transfer and the Fermi level shift. These findings could provide useful information for designing novel high-performance Schottky devices.

4. Conclusion

In summary, we have systematically investigated the structural and electronic properties of the graphene/GaS vdWH as well as the effect of electric gating by using density functional theory. The interlayer distance of 3.356 Å and the negative value of the binding energy per carbon atom in the vdWH suggest that the weak vdW interactions are dominated between the graphene and the monolayer GaS in the heterostructure. Interestingly, the graphene/GaS vdWH forms an *n*-type Schottky contact with the SBH of 0.52 eV at the equilibrium state. Both the contact types and the SBH in the graphene/GaS vdWH can be induced by applying the electric field, which can also effectively modulate the electronic properties of the heterostructure. When the negative electric field is larger than −3 V/nm, a transformation of the contact types from the Schottky contact to Ohmic one are observed, whereas when the positive electric field is larger than +3 V/nm, a transition of the Schottky contact from the *n*-type to the *p*-type occurs. Thus, we expect that the graphene/GaS vdWH can be considered to be a promising alternative material for future nano- and opto-devices.

Acknowledgements

This research is funded by Vietnam National Foundation for Science and Technology Development (NAFOSTED) under grant number 103.01-2016.07.

References

[1] M. Xu, T. Liang, M. Shi, H. Chen, Graphene-like two-dimensional materials, Chem. Rev. 113 (2013) 3766–3798.
[2] G. Fiori, F. Bonaccorso, G. Iannaccone, T. Palacios, D. Neumaier, A. Seabaugh, S.K. Banerjee, L. Colombo, Electronics based on two-dimensional materials, Nat. Nanotechnol. 9 (2014) 768–779.
[3] F. Schwierz, J. Pezoldt, R. Granzner, Two-dimensional materials and their prospects in transistor electronics, Nanoscale 7 (2015) 8261–8283.
[4] K.S. Novoselov, A.K. Geim, S. Morozov, D. Jiang, M. Katsnelson, I. Grigorieva, S. Dubonos, A. Firsov, Two-dimensional gas of massless Dirac fermions in graphene, Nature 438 (2005) 197–200.
[5] A.C. Neto, F. Guinea, N.M. Peres, K.S. Novoselov, A.K. Geim, The electronic properties of graphene, Rev. Mod. Phys. 81 (2009) 109–162.
[6] M. Sprinkle, D. Siegel, Y. Hu, J. Hicks, A. Tejeda, A. Taleb-Ibrahimi, P. Le Fèvre, F. Bertran, S. Vizzini, H. Enriquez, S. Chiang, P. Soukiassian, C. Berger, W.A. de Heer, A. Lanzara, E.H. Conrad, First direct observation of a nearly ideal graphene band structure, Phys. Rev. Lett. 103 (2009) 226803–226806.
[7] Y. Li, Z. Zhou, S. Zhang, Z. Chen, MoS_2 nanoribbons: high stability and unusual electronic and magnetic properties, J. Am. Chem. Soc. 130 (49) (2008) 16739–16744.
[8] B. Radisavljevic, A. Radenovic, J. Brivio, i. V. Giacometti, A. Kis, Single-layer MoS_2 transistors, Nat. Nanotechnol. 6 (2011) 147–150.
[9] C.V. Nguyen, N.N. Hieu, N.A. Poklonski, V.V. Ilyasov, L. Dinh, T.C. Phong, L.V. Tung, H.V. Phuc, Magneto-optical transport properties of monolayer MoS_2 on polar substrates, Phys. Rev. B 96 (2017) 125411–125424.
[10] R. Ganatra, Q. Zhang, Few-layer MoS_2: a promising layered semiconductor, ACS Nano 8 (2014) 4074–4099.
[11] C.V. Nguyen, N. Ngoc Hieu, C. Duque, D. Quoc Khoa, N. Van Hieu, L. Van Tung, H. Vinh Phuc, Linear and nonlinear magneto-optical properties of monolayer phosphorene, J. Appl. Phys. 121 (2017) 045107–045112.
[12] E.S. Reich, Phosphorene excites materials scientists, Nature 506 (2014) 19.
[13] H.V. Phuc, N.N. Hieu, V.V. Ilyasov, L.T. Phuong, C.V. Nguyen, First principles study of the electronic properties and band gap modulation of two-dimensional phosphorene monolayer: effect of strain engineering, Superlattice. Microst. 118 (2018) 289–297.
[14] S. Zhang, M. Xie, F. Li, Z. Yan, Y. Li, E. Kan, W. Liu, Z. Chen, H. Zeng, Semiconducting group 15 monolayers: a broad range of band gaps and high carrier mobilities, Angew. Chem. 128 (2016) 1698–1701.
[15] D.V. Rybkovskiy, A.V. Osadchy, E.D. Obraztsova, Transition from parabolic to ring-shaped valence band maximum in few-layer GaS, GaSe, and InSe, Phys. Rev. B 90

(2014) 235302–235310.
[16] M. Yagmurcukardes, R. Senger, F. Peeters, H. Sahin, Mechanical properties of monolayer GaS and GaSe crystals, Phys. Rev. B 94 (2016) 245407–245413.
[17] Y. Ma, Y. Dai, M. Guo, L. Yu, B. Huang, Tunable electronic and dielectric behavior of GaS and GaSe monolayers, Phys. Chem. Chem. Phys. 15 (2013) 7098–7105.
[18] G. Shen, D. Chen, P.-C. Chen, C. Zhou, Vapor- solid growth of one-dimensional layer-structured gallium sulfide nanostructures, ACS Nano 3 (2009) 1115–1120.
[19] H.L. Zhuang, R.G. Hennig, Single-layer group-III monochalcogenide photocatalysts for water splitting, Chem. Mater. 25 (2013) 3232–3238.
[20] D.J. Late, B. Liu, J. Luo, A. Yan, H.R. Matte, M. Grayson, C. Rao, V.P. Dravid, Gas and gase ultrathin layer transistors, Adv. Mater. 24 (2012) 3549–3554.
[21] K. Roy, M. Padmanabhan, S. Goswami, T.P. Sai, G. Ramalingam, S. Raghavan, A. Ghosh, Graphene-MoS_2 hybrid structures for multifunctional photoresponsive memory devices, Nat. Nanotechnol. 8 (2013) 826–830.
[22] H. Coy Diaz, J. Avila, C. Chen, R. Addou, M.C. Asensio, M. Batzill, Direct observation of interlayer hybridization and Dirac relativistic carriers in graphene/MoS_2 van der Waals heterostructures, Nano Lett. 15 (2015) 1135–1140.
[23] W. Kim, C. Li, F.A. Chaves, D. Jiménez, R.D. Rodriguez, J. Susoma, M.A. Fenner, H. Lipsanen, J. Riikonen, Tunable graphene–GaSe dual heterojunction device, Adv. Mater. 28 (2016) 1845–1852.
[24] Z. Ben Aziza, H. Henck, D. Pierucci, M.G. Silly, E. Lhuillier, G. Patriarche, F. Sirotti, M. Eddrief, A. Ouerghi, Van der waals epitaxy of gase/graphene heterostructure: electronic and interfacial properties, ACS Nano 10 (2016) 9679–9686.
[25] R. Lu, J. Liu, H. Luo, V. Chikan, J.Z. Wu, Graphene/GaSe-nanosheet hybrid: towards high gain and fast photoresponse, Sci. Rep. 6 (2016) 19161–19167.
[26] C. Jin, F.A. Rasmussen, K.S. Thygesen, Tuning the Schottky barrier at the graphene/MoS_2 interface by electron doping: density functional theory and many-body calculations, J. Phys. Chem. C 119 (2015) 19928–19933.
[27] J. Padilha, A. Fazzio, A.J. da Silva, Van der waals heterostructure of phosphorene and graphene: tuning the Schottky barrier and doping by electrostatic gating, Phys. Rev. Lett. 114 (2015) 066803–066807.
[28] M. Sun, J. Chou, J. Yu, W. Tang, Electronic properties of blue phosphorene/graphene and blue phosphorene/graphene-like gallium nitride heterostructures, Phys. Chem. Chem. Phys. 19 (2017) 17324–17330.
[29] H.V. Phuc, V.V. Ilyasov, N.N. Hieu, B. Amin, C.V. Nguyen, Van der waals graphene/g-GaSe heterostructure: tuning the electronic properties and Schottky barrier by interlayer coupling, biaxial strain, and electric gating, J. Alloy. Compd. 750 (2018) 765–773.
[30] H.V. Phuc, N.H. Nguyen, B.D. Hoi, C.V. Nguyen, Interlayer coupling and electric field tunable electronic properties and Schottky barrier in graphene/bilayer-GaSe van der waals heterostructure, Phys. Chem. Chem. Phys. 20 (2018) 17899–17908.
[31] G.W. Mudd, S.A. Svatek, L. Hague, O. Makarovsky, Z.R. Kudrynskyi, C.J. Mellor, P.H. Beton, L. Eaves, K.S. Novoselov, Z.D. Kovalyuk, E.E. Vdovin, A.J. Marsden, N. Wilson, A. Patane, High broad-band photoresponsivity of mechanically formed InSe–graphene van der waals heterostructures, Adv. Mater. 27 (2015) 3760–3766.
[32] W. Luo, Y. Cao, P. Hu, K. Cai, Q. Feng, F. Yan, T. Yan, X. Zhang, K. Wang, Gate tuning of high-performance InSe-Based Photodetectors using graphene electrodes, Adv. Opt. Mater. 3 (2015) 1418–1423.
[33] K.D. Pham, N.N. Hieu, V.V. Ilyasov, H.V. Phuc, B.D. Hoi, E. Feddi, N.V. Thuan, C.V. Nguyen, First principles study on the electronic properties and Schottky barrier of Graphene/InSe heterostructure, Superlattice. Microst. 516 (2018) 213–217.
[34] P. Giannozzi, S. Baroni, N. Bonini, M. Calandra, R. Car, C. Cavazzoni, D. Ceresoli, G.L. Chiarotti, M. Cococcioni, I. Dabo, A.D. Corso, S. de Gironcoli, S. Fabris, G. Fratesi, R. Gebauer, U. Gerstmann, C. Gougoussis, A. Kokalj, M. Lazzeri, L. Martin-Samos, N. Marzari, F. Mauri, R. Mazzarello, S. Paolini, A. Pasquarello, L. Paulatto, C. Sbraccia, S. Scandolo, G. Sclauzero, A.P. Seitsonen, A. Smogunov, P. Umari, R.M. Wentzcovitch, Quantum espresso: a modular and open-source software project for quantum simulations of materials, J. Phys. Condens. Matter 21 (2009) 395502–395520.
[35] P.E. Blöchl, Projector augmented-wave method, Phys. Rev. B 50 (1994) 17953–17979.
[36] J.P. Perdew, K. Burke, M. Ernzerhof, Perdew, burke, and ernzerhof reply, Phys. Rev. Lett. 80 (1998) 891–891.
[37] S. Grimme, Semiempirical GGA-type density functional constructed with a long-range dispersion correction, J. Comput. Chem. 27 (2006) 1787–1799.
[38] A. Woessner, M.B. Lundeberg, Y. Gao, A. Principi, P. Alonso-González, M. Carrega, K. Watanabe, T. Taniguchi, G. Vignale, M. Polini, J. Hone, R. Hillenbrand, F. Koppens, Highly confined low-loss plasmons in graphene–boron nitride heterostructures, Nat. Mater. 14 (2015) 421–425.
[39] C. Si, Z. Lin, J. Zhou, Z. Sun, Controllable Schottky barrier in GaSe/graphene heterostructure: the role of interface dipole, 2D Mater. 4 (2016) 015027–015033.
[40] F. Zhang, W. Li, Y. Ma, X. Dai, Schottky barrier tuning of the graphene/SnS_2 van der waals heterostructures through electric field, Solid State Commun. 271 (2018) 56–61.
[41] M. Sun, J.-P. Chou, Q. Ren, Y. Zhao, J. Yu, W. Tang, Tunable Schottky barrier in van der waals heterostructures of graphene and g-GaN, Appl. Phys. Lett. 110 (2017) 173105–173108.
[42] J. Bardeen, Surface states and rectification at a metal semi-conductor contact, Phys. Rev. 71 (1947) 717–727.